



Permanent and Transient Electrophysiological Effects During Cardiac Cryoablation Documented by Optical Activation Mapping and Thermal Imaging

Gregory E. Morley,

Division of Cardiology, New York University School of Medicine.

Scott A. Bernstein,

Division of Cardiology, New York University School of Medicine.

Laura M. Kuznekoff,

Division of Cardiology, New York University School of Medicine.

Carolina Vasquez,

Division of Cardiology, New York University School of Medicine.

J. Philip Saul,

West Virginia University, School of Medicine.

Dieter Haemmerich* [Senior Member IEEE]

Dept. of Pediatrics, Medical Univ. of South Carolina.

Abstract

Objective: Cardiac catheter cryoablation is a safer alternative to radiofrequency ablation for arrhythmia treatment, but electrophysiological (EP) effects during and after freezing are not adequately characterized. The goal of this study was to determine transient and permanent temperature induced EP effects, during and after localized tissue freezing.

Methods: Conduction in right (RV) and left ventricles (LV) was studied by optical activation mapping during and after cryoablation in paced, isolated Langendorff-perfused porcine hearts. Cryoablation was performed endocardially (n=4) or epicardially (n=4) by a cryoprobe cooled to -120°C for 8 minutes. Epicardial surface temperature was imaged with an infrared camera. Viability staining was performed after ablation. Motion compensation and co-registration was performed between optical mapping data, temperature image data, and lesion images.

Results: Cryoablation produced lesions 14.9 ± 3.1 mm in diameter and 5.8 ± 1.7 mm deep. A permanent lesion was formed in tissue cooled below $-5 \pm 4^{\circ}\text{C}$. Transient EP changes observed at temperatures between 17 and 37°C during cryoablation surrounding the frozen tissue region directly correlated with local temperature, and include action potential (AP) duration prolongation, decrease in AP magnitude, and slowing in conduction velocity ($Q_{10}=2.0$). Transient conduction block was observed when epicardial temperature reached $<17^{\circ}\text{C}$, but completely resolved upon tissue rewarming, within 5 minutes.

*correspondence haemmer@musc.edu.

Conclusion: Transient EP changes were observed surrounding the permanent cryo lesion ($< -5\text{ }^{\circ}\text{C}$), including conduction block (-5 to $17\text{ }^{\circ}\text{C}$), and reduced conduction velocity ($>17\text{ }^{\circ}\text{C}$).

Significance: The observed changes explain effects observed during clinical cryoablation, including transient increases in effective refractory period, transient conduction block, and transient slowing of conduction. The presented quantitative data on temperature dependence of EP effects may enable the prediction of the effects of clinical cryoablation devices.

Keywords

Cardiac catheter ablation; cryoablation; cryotherapy

I. Introduction

Cardiac catheter cryoablation has become an alternative to radiofrequency (RF) ablation, and has found considerable interest particularly in pediatric patients [1-3] due to several safety advantages: (1) no risk of steam popping and lower risk of thrombus formation [4], (2) no risk of coronary vessel stenosis [5-7], (3) adherence of the catheter to the target site upon freezing, and (4) cryo-mapping allows confirmation of target site before creating a permanent lesion, which is of particular importance when the target site is close to sensitive structures (e.g. the AV node) [1, 8]. One particular shortcoming of cryo compared to RF ablation is the comparably higher incidence of recurrences (i.e. late recovery of tissue function), which can occur anywhere from immediately post cryoablation to a few minutes to days later [1, 3, 9-12]. The use of larger cryocatheter tips, more applications (freeze-thaw-freeze) and more aggressive locations for septal substrates has led to reduced late recurrences [12]; however, early recurrences after apparently successful ablations remain frustrating and often perplexing. A number of transient effects during and after cryoablation have been described in the literature, including conduction block [1], a prolongation of the effective refractory period [2], and a reduction in electrogram magnitude [13, 14]. A better understanding of the local electrophysiological (EP) changes resulting from tissue cooling and freezing may aid in explaining these clinical observations, and help in designing more effective cryoablation devices. While prior studies have examined the effects of hypothermia on EP changes in perfused tissue [15-17], these studies employed uniform cooling of the preparation to temperatures above freezing, and did not include the creation of permanent lesions. There have not been any prior studies demonstrating the EP changes surrounding a cryo probe, while correlating these changes with local tissue temperature.

In this study we employed optical activation mapping during and after cryoablation on a perfused porcine heart model while thermally imaging the epicardial surface. This allowed for simultaneous measurement of spatio-temporal temperature profile and EP changes during local tissue freezing, which is not possible *in vivo*. The goal of this study was to correlate EP changes with temperature to clinically explain observed effects as well as to quantify the changes with corresponding tissue temperatures.

II. Methods

A. Animals

The study was performed using four healthy Yorkshire pigs, weighing between 40 and 60 kg. All animal care protocols conformed to institutional and NIH guidelines, and were approved by the Institutional Animal Use and Care Committee at the authors' institution.

B. Extraction and Langendorff Perfusion

Pigs were brought to the operating room in the fasted state, sedated and intubated (propofol 2.5-3.5 mg/kg, isoflurane 1-5%). A median sternotomy was performed and the great vessels were identified. The pericardium was then incised. After the heart was exposed, animals were given intravenous heparin (15,000 IU) and an overdose of sodium pentobarbital (120 mg/kg; Sleepaway, Fort Dodge Animal Health, Fort Dodge, IA) for euthanasia. The inferior and superior vena cava were cross-clamped and ventricular fibrillation was induced with 9V direct current. The great vessels were cut and hearts were rinsed with room-temperature Tyrode's solution and transported on ice. Hearts were perfused at a constant pressure of 60 mmHg antegradely via the ascending aorta with a modified Tyrode's solution containing the excitation contraction uncoupler blebbistatin (5 μ M), at physiologic flow rates and temperature. The Tyrode's solution was not recirculated. Hearts regained sinus rhythm within 10 minutes and did not require defibrillation. A cannula was inserted through the left atria into the left ventricle to prevent pressure from accumulated fluid in the left ventricle. Hearts were suspended in room temperature air to allow for thermal imaging and all experiments were completed within 1 hour.

C. Optical Mapping and ECG Recording

Hearts were optically mapped similar to prior studies [18], using the voltage sensitive dye, di-4-ANEPPS (Invitrogen-Molecular Probes, Carlsbad, CA). Four custom-mounted green (530 nm) LED arrays (Luxeon Inc, San Jose, CA) were used as light source. Emitted light was detected with a high-resolution charge-coupled device (CCD) camera (128 \times 128 pixels, Dalsa Semiconductor Corp, Bromont, Quebec) through >610 nm filters. The images were digitally captured at a sample rate of 400 frames/second and stored for later analysis using custom software. Volume-conducted whole-heart electrograms were obtained with submerged electrodes and continuously recorded during optical mapping (AxoScope, DigiData, Molecular Devices, Inc, Sunnyvale, California). Epicardial pacing was performed at a constant cycle length of 400 ms using a 6 French quadripolar diagnostic electrophysiology catheter (CRD Response, St Jude Medical, Inc. St. Paul, MN) and a Pulsar 6i stimulator (FHC, Bowdoinham, ME).

D. Cryoablation

Three to five fiducial markers were placed surrounding the location of intended cryoablation to provide spatial reference points for later analysis. We performed cryoablation for 8 min with a 5 mm diameter probe (Cry-Ac, Brymill, Ellington, CT) perfused with liquid nitrogen resulting in a probe temperature of approximately -120 °C. Compared to clinical cryoablation devices, our probe had a larger tip diameter and lower tip temperature with the

goal of creating larger cryo lesions. The reason for this choice was (1) to achieve reproducible transmural lesions, and (2) to achieve reduced radial temperature gradients. The latter was necessary to allow direct correlation between temperature and EP parameters. For endocardial cryo applications, the cryo catheter was steered within either the right ventricle (RV) or left ventricle (LV) towards the target location by tactile guidance, and cryoablation was performed from the endocardial side in the free wall of either RV (n=2), or LV (n=2). For epicardial cryo applications, the cryo catheter was visually positioned at the epicardial target location on either RV (n=3) or LV (n=1) free wall.

E. Thermal imaging

Epicardial surface temperature was imaged at a frame rate of 1/s during, and 15 min following cryoablation with an infrared camera (Mikron M7500; wavelength 8-14 μm ; 320 \times 240 resolution). Temperature was calibrated with an internal source before initiating recording, with measurement accuracy of ± 2 $^{\circ}\text{C}$. To determine the surface temperature of a material when recording the emitted infrared spectrum, the emissivity of the material has to be known to convert infrared emissions to temperature; for epicardium we assumed a tissue emissivity of 0.9 [19]. The field of view (FOV) of both the optical mapping camera, as well as the infrared camera was adjusted so that the cryo probe was centered, and the total FOV was at least $\sim 3 \times 3$ cm.

F. Gross Pathology

After the studies were completed, tissue samples containing the lesions were extracted. Digital images of the lesion surfaces, as well as of lesion crosssection after slicing the tissue with a scalpel were acquired, and were used to define extent of permanent lesions produced by the cryoablations. In preliminary studies we confirmed that the lesion visible without staining (Fig. 2) coincides with the lesion defined by viability staining via nitro-blue tetrazoleum (data not shown). Lesion diameter and depth were measured, similar to prior studies [20].

G. Data processing

All image processing was performed by custom software code developed within Matlab (Mathworks, Natick, MA).

1) Optical Activation Mapping: As first step we performed motion compensation of the optical mapping movies to correct for residual motion that was present after administration of the excitation contraction uncoupler. All subsequent image frames were registered to the first frame via 2D affine transformation such that fiducial marker locations were matched. As second step, we performed temporal averaging over all cardiac cycles present in each of the data sets (typically ~ 8 cycles). Subsequently, an image processing technique called HYPR was applied, which enhances the SNR in a temporal image series [21]. Additionally, a Gaussian filter and median filter (3 \times 3 kernel) were applied to further reduce noise. From these data we calculated time of activation, action potential (AP) amplitude, action potential duration (APD90), and conduction velocity. Conduction velocity of each pixel was calculated based on the activation times of an array of the neighboring 5 \times 5 pixels as described in prior studies [18].

2) Registration of Image Data Sets: To co-localize (1) optical mapping data, (2) thermal imaging data, and (3) lesion images, we had to perform registration of these three image data sets. During this procedure, any necessary translation, rotation and perspective correction was performed on the image data sets such that the data can be spatially correlated (Fig. 1). We used the fiducial markers (visible in all three data sets) placed on the epicardial surface before the cryoablation to provide reference locations for performing the geometrical transformation. We wrote custom software algorithms in Matlab (Mathworks, Natick, MA) to perform 2D affine transformation on the thermal imaging data, and on the lesion images to register those to the optical imaging data sets. Fig. 1 demonstrates the registration process.

Based on the registered image data sets we determined the temperature required for permanent lesion formation by correlating the temperature profile at the end of the cryoablation with the lesion boundaries extracted from lesion images. From correlation between optical mapping signal data registered to temperature data we determined:

- Action potentials at different temperatures by averaging the optical mapping signals of all tissue regions that are at this particular temperature
- Temperature dependence of both APD90 and conduction velocity

For the latter two correlations, we divided the temperature range from 22 – 37 °C into 5 °C intervals (bins), and calculated average and standard deviation in each temperature interval.

III. Results

Table 1 summarizes parameters of each of the eight cryo applications. Three cryoablations in the RV resulted in transmural lesions, the remainder five lesions were nontransmural. Lesions were on average 14.9 +/- 3.1 mm in diameter and 5.8 +/- 1.7 mm deep. Epicardial lesions had a larger diameter of 17.1 +/- 2.4 mm, compared to 12.8 +/- 2.3 mm for endocardial lesions ($p < 0.05$), but lesion depth was not significantly different ($p = 0.84$). The duration required for epicardial tissue rewarming following a cryo application was significantly longer for epicardial (6.3 +/- 1.5 min) compared to endocardial (2.5 +/- 1.0 min) application ($p < 0.05$); note that contrary to epicardial applications, for endocardial applications the location of lowest temperature could not be assessed. The rewarming time of epicardial applications is thus likely more representative of the time required for the lesion to completely rewarm.

Fig. 2 shows a non-transmural LV lesion (A,B), and a transmural RV lesion (C,D), both following endocardial cryo application (Lesions Endo1 and Endo2 in Table 1). The non-transmural lesion has the tear-drop shape (Fig. 2A) often seen also for radiofrequency lesions, while the transmural lesion is approximately cylindrical (Fig. 2C,D). Lesion boundaries were clearly demarcated.

Fig. 3 compares transient and permanent changes in epicardial activation, resulting from a non-transmural, and from a transmural cryo lesion (both applied endocardially). Transient changes from a non-transmural lesion (Lesion Endo1; see Fig. 2A,B) are demonstrated in

activation maps (A-D), and corresponding temperature maps (E-F) before, during and after a cryoablation (see also 3). Transient as well as permanent changes were observed from a transmural lesion (Lesion Endo2; see Fig. 2C,D) with activation maps (G-J) and corresponding temperature data (K,L) (see also Suppl. Movie 2). Due to the latent heat associated with the state change of tissue water between liquid and frozen, the temperature time course shows discontinuities at the time points freezing and thawing occurs (K, arrows). For the transmural lesion, activation time of location of latest activation at end of cryoablation (purple region in Fig. 3I) was retarded by 21.0 ms, compared to initial activation time (Fig. 3G). Following tissue rewarming (Fig. 3J), activation stayed retarded by 9.3 ms compared to initial activation time. For lesions created by epicardial cryo application, the observed change in activation timing and presence of a transient late activation zone was equivalent to that of the transmural lesions resulting from endocardial application. We only present activation maps resulting from endocardial but not epicardial cryo applications due to higher clinical significance, and because the epicardial surface was partially obscured by the cryo catheter for epicardial cryo applications.

Activation time of location of latest activation at end of cryoablation was retarded on average by 19.5 ± 11.3 ms, compared to initial activation time ($p < 0.01$). Following tissue rewarming, activation timing was not significantly different from initial timing ($p = 0.75$), though in two individual lesions we observed permanent altered activation (Table 1). The observed retardation was not significantly different between endocardial and epicardial cryo applications ($p = 0.92$).

Correlation of temperature data with conduction velocity (A) and APD90 (B) are shown in Fig. 4 As measure of the temperature sensitivity of conduction velocity we calculated $Q_{10} = v_T / v_{T+10^\circ\text{C}}$, where v_T is conduction velocity at temperature T. The relationship between conduction velocity and temperature could be modeled adequately by a linear equation between $20 - 37^\circ\text{C}$ ($R^2 = 0.97$). Based on this linear mathematical model, we defined appearance of conduction block where conduction velocity is estimated to be equal to zero, which would occur at a temperature of 17°C (Fig. 4C).

Fig. 5 demonstrates changes in action potential morphology surrounding the cryo lesion during, and after cryoablation. A few minutes after thawing, the permanent lesion becomes visible with boundary just inside where the iceball boundary was located (B, arrows). At the end of cryoablation, signal magnitude is reduced even at the furthest location from the iceball (E, yellow curve) compared to pre-ablation (E, white dotted curve) due to reduced tissue temperature of 29°C , but returns to pre-ablation levels after tissue has rewarmed (F). The corresponding signal magnitude profile as measured between baseline and plateau (white double arrow in (E)) of the optical signal in (E,F), is shown in gray-scale images (C,D). Note that temperature does not affect dye sensitivity, as prior studies have used voltage sensitive dyes at lower temperatures [22], and they have been used for squid axon recordings down to 4°C without degradation in voltage sensitivity. (G)-(H) shows maps of action potential duration (APD90) surrounding the target site before, during, and after freezing.

IV. Discussion

The most important new findings of this study are that: 1) there are local electrophysiological (EP) effects from cryoablations, including conduction block and changes in conduction velocity and action potential morphology that help explain multiple observations during clinical cryoablation procedures, and 2) the transient nature of these changes when the cryoablation does not result in a permanent lesion may explain transient clinical effects, such as early recurrence of conduction and arrhythmias after an apparently successful cryoablation procedure. Further, the presented quantification of the EP effects and corresponding temperature ranges may enable design of more effective cryoablation devices.

While cardiac cryosurgery has been studied for decades [14, 23], cardiac catheter cryoablation has received increased attention only within the recent years, particularly for treatment of pediatric patients due to several safety advantages over RF ablation [1-3, 24]. However, the primary disadvantage of clinical cryoablation has been transient, rather than permanent EP effects, which lead to recurrence of both conduction in the targeted substrate and arrhythmias. In this study, simultaneous optical activation mapping was combined with thermal imaging to locally correlate temperature with resulting EP changes at and around the cryoablation site after spatial registration of the data sets. Cryoablation was performed for 8 min at -120°C tip temperature (5 mm diameter tip) both by endo- and epicardial application, which created cryo lesions somewhat larger than seen typically with clinical devices that operate only at -80°C . We used the larger tip and lower temperature to generate wider hypothermic tissue regions with less steep temperature gradients, allowing accurate correlation of local temperature with optical mapping data. Depending mostly on myocardial thickness at the target location, both transmural and non-transmural lesions were created (Fig. 2). Lesions resulting from endocardial applications were smaller in diameter than epicardial lesions (Table 1), likely resulting from convective warming by perfusate at the endocardial surface [20]. During a cryoablation that resulted in a non-transmural lesion (Fig. 2A,B), transient functional conduction block was observed at the epicardial location that coincided with location of lowest temperature of around 17°C (Fig. 3B,E). This conduction block disappeared upon rewarming of the tissue after ablation was discontinued (Fig. 3C,F) (see Suppl. Movie 2). Thus, there is a transient loss of tissue function that is completely reversible as long as no permanent lesion is formed, i.e. in the temperature range of -5°C to 17°C . A similar conduction block was observed at the beginning of a cryoablation that later resulted in a transmural lesion (Fig. 3H) (see Suppl. Movie 1), at the location where the permanent lesion was subsequently created once the ice ball formed (Fig. 3I).

Clinically, the effect of temporary loss of conduction during cryoablation and its use to identify target sites during catheter ablation is termed cryo-mapping, and was first described by Gessman et al [25], though earlier cryosurgery studies noted reversible loss of conduction when cooling tissue to 0°C [23]. Some clinical cryo systems have a mapping mode by setting catheter tip temperature to a higher temperature (typically -30°C , instead of -80°C for ablation). Ideally the tissue volume transiently deactivated during cryo-mapping coincides with the volume where a permanent cryo lesion is created during ablation, but from our experience this is often not the case. The quantitative data on the temperature ranges of different tissue effects (Fig. 6) will enable better matching mapping and lesion

volume when designing new cryoablation devices. In addition, the phenomenon of mapping takes place at all tip temperature settings (i.e. during both mapping and ablation) due to the temperature gradient surrounding the cryo probe; i.e. a zone of mapping precedes any areas of eventual cell death (Fig. 6). The clinical problem is that since the spatiotemporal temperature profile is unknown during a clinical procedure, there is no easy way to differentiate mapping effects from permanent ablation effects. This issue is particularly important when the mapping effects last more than a few minutes, because the procedure may be assumed successful and concluded, only to have the arrhythmia recur later.

Our observation of prolonged conduction block is consistent with the clinical observations of variably delayed conduction recurrence in the target tissue. For instance, transient AV conduction block is observed commonly during cryoablation near the AV node [1]. In this study, transient conduction block occurred once tissue cooled to 17 °C. For comparison, prior hypothermia studies where perfused rabbit hearts were uniformly cooled showed AV block in the range of 17 – 27 °C, and complete loss of excitability at 12 °C [15]. An earlier study found loss of atrial excitability at 18 °C [17].

In addition to conduction block, transient slowing in conduction was observed at the epicardium preceding, and surrounding the site of transient conduction block (Fig. 3B). Similarly, when a permanent lesion was created, regions of transient conduction slowing surrounded the permanent lesion site during cryoablation (Fig. 3I). There was a direct correlation between conduction velocity and temperature with a drop to about 50% for every ten degrees temperature reduction ($Q_{10} = 2.0$) (Fig. 4A), which is in the same range as in prior hypothermia studies where perfused hearts were uniformly cooled [16]. Based on the relationship between temperature and conduction velocity (Fig. 4C), we estimated conduction block (defined as where conduction velocity would reach zero) to occur below 17 °C; this is in agreement with the qualitative observation of conduction block at ~17 °C based on Fig. 3B and 3E.

As a result of conduction slowing, the location of latest activation was distal to the cryo lesion with reference to the pacing site (Fig. 3J). After cessation of cryoablation, the tissue required ~2-9 minutes to warm back to body temperature, during which there was slow recovery of normal conduction (Fig. 3C,D; Fig. 3I,J). While in the majority of the cases activation timing was equivalent to that before ablation following rewarming (Fig. 3A,D), in two cases activation timing stayed retarded up to the end of the observation period (15 min after cryoablation) (Table 1). The transient slowing of cardiac conduction during cryoablation, observed clinically both for accessory pathways and the AV node [26, 27], can be explained by these direct effects of temperature on conduction velocity.

At three locations in the right ventricle, transmural lesions could be created with an almost cylindrical shape (see Fig. 2C,D) with epicardial temperatures that reached below -20 °C at the lesion center (Fig. 3K,L). The correlation between temperature data and the visual lesion boundary after ablation suggests that a minimum temperature of -5 +/- 4 °C is required for a permanent lesion to form, which is slightly below the threshold temperature where tissue freezes (-2 to -3 °C). This is in agreement with a prior *in vivo* canine study that found the permanent lesion to be located 1.5 - 2.5 mm inside the visible ice ball, with no change in

lesion size within 4 weeks relative to acute lesion size [28]. It is thus possible that the extent of the frozen tissue region could be used to define the permanent lesion, perhaps by visualizing it with a technologies like ultrasound imaging [29].

In general, the changes in activation timing and development of a region of late activation distal to the transmural lesion relative to the pacing site are similar to the observations in the non-transmural lesion in the LV described earlier. The temperature-related delay in restoration of tissue function due to the 2 – 9 min rewarming period to body temperature (Fig. 3K) may explain some of the arrhythmia recurrences that have been clinically observed early after ablation. Note however that the lesions created in our model are larger due to a lower cryo probe temperature (-120°C) than that used clinically. Thus, the tissue rewarming time is likely shorter following clinical ablations than shown here.

In addition to the temperature dependent changes in conduction velocity (Fig. 4A), transient changes in action potential morphology were observed as a result of tissue cooling. These changes include action potential prolongation (Fig. 4B), reduced rates of depolarization and repolarization, as well as a reduction in amplitude (Fig. 5). It is reasonable to assume that action potentials are not actively generated within the iceball. The signals detected within the iceball are therefore likely electrotonically propagated [30]. This is in agreement with prior reports, where electrograms of reduced magnitude and deflection were measured by electrodes placed on acute, as well as 4 week old cryo lesions [14]. The effects of tissue freezing on the action potential are however not relevant to clinical cryoablation because once the iceball forms around the catheter tip, the ability to measure any electrical signal from the catheter is eliminated as ice is electrically insulating.

In addition to the permanent loss of tissue function inside the cryo lesion, the appearance of transient conduction block below 17°C suggests transient loss of tissue function directly outside the ice ball (i.e. between -5 and 17°C); this temperature is in agreement with prior studies that found complete loss of excitability between 12 and 18°C [15, 17]. Thus, tissue below 17°C also presumably does not generate action potentials and the observed signals below that temperature represent electrotonic decay.

The cooling induced action potential prolongation was quantified here via APD90. Due to the temperature gradient present during cryoablation where lowest temperatures are at the center, the APD90 was highest close to the iceball (and permanent lesion) and progressively decreased with distance from the iceball (Fig. 5H). The APD correlates with the effective refractory period (ERP), and a prior animal study showed a local increase in ERP in left ventricles that were locally cooled from the epicardial side [31]. In addition, there are clinical reports that have shown a transient increase of the ERP of the fast AV nodal pathway during cryoablation in patients with AV-node reentrant tachycardia (AVNRT), with return to baseline after ablation [2]. Presumably, this transient increase in fast pathway ERP is due to temperature related changes in the APD of the fast pathway and/or His bundle during cryoapplication in the area of the slow pathway that occur when the catheter is relatively near the anterior AV node. These results are also in agreement with prior studies, where similar APD prolongation and changes in AP morphology has been documented in

hypothermia studies [15, 16]. The observed APD changes were transient suggesting a direct relationship to tissue temperature (Fig. 4B).

The observed changes in AP morphology (Fig. 5E) may be explained by the temperature dependence of ion channel conductances. Many ion channels, including Na, K and Ca channels, exhibit reduced ion channel conductance at hypothermic temperatures [32-34]. In particular, lower AP amplitude and lower rate of depolarization may be attributed to a reduction in Na channel conductance, while delay and reduced slope of repolarization may be due to reduced K channel conductance. Reduced Na channel conductance has been suggested as one of the factors responsible for slowing in conduction velocity in prior hypothermia studies [15]. In addition, it is known that gap junction conductance decreases during hypothermia [35], which is another factor that lowers conduction velocity [15, 36]. These observed decreases in channel and gap junction conductances are in part due to reduced molecular motion at lower temperatures - particularly motion of ions and water molecules - as described by Brownian dynamics [37, 38]. The observed temperature dependence of AP morphology (e.g. APD90) and conduction velocity (Fig. 4) is thus likely in both cases the result of the temperature dependent changes in ion channel conductances [36].

Based on the observations above, we can identify three distinct temperature ranges, each associated with specific EP effects: (1) transient conduction slowing and changes in AP morphology (17 - 37 °C), (2) transient loss of tissue function (i.e. conduction block) (-5 to 17 °C), and (3) permanent loss of tissue function (i.e. cryo lesion) (below -5 °C). During cryoablation, a certain tissue location may pass through one or more of these three temperature ranges as tissue cools down. In addition, all three temperature ranges are usually simultaneously present surrounding a cryo probe (Fig. 6). In this study we presented the temporal and spatial dynamics that occur during cryoablation involving these three temperature ranges and quantified the corresponding EP effects. The operator should be aware of these dynamic changes during freezing; for example the rapidity at which EP changes (e.g. disappearance of the ablation catheter signal) are observed following initiation of freezing may serve as predictor of successful cryo applications.

Since the presented observations are based on a perfused non-working heart model, there are several factors that deviate from clinical cryoablation: (1) we used a different cryoablation device (lower temperature, larger tip), (2) endocardial perfusion with blood may behave differently from *ex vivo* perfusate, and (3) the blood inside the heart chamber represents a large heat source that will likely affect tissue temperatures significantly. While we assume here that the presented temperature dependence of EP effects is similar during clinical cryoablation, the specific spatial and temporal dynamics likely deviate from the results presented here. However, it may be feasible to extrapolate spatial and temporal EP changes during clinical cryoablations based on temperature profiles of clinical cryoablation devices using the herein presented results.

V. Conclusions

A number of electrophysiological (EP) changes result from tissue cooling during cardiac cryoablation. Transient changes around the site of cryoablation include conduction block, reduced conduction velocity, action potential prolongation, decrease in action potential magnitude. These changes can explain several of the effects observed during clinical cryoablation, including transient increases in ERP, transient conduction block, and transient slowing of conduction. In addition, delayed tissue rewarming may explain delayed recovery of tissue function after cryoablation.

Based on our observations, we could identify three temperature ranges, each associated with specific EP effects (Fig. 6). The presented quantification of the temperature and resulting permanent and transient EP changes is relevant for designing new cryoablation devices, since these data will allow engineers to predict what transient and permanent effects a particular device with a specific thermal profile will produce.

Supplementary Material

Refer to Web version on PubMed Central for supplementary material.

Acknowledgments

This work was supported by grants HL076751 (to G.E.M.) from the NIH. Part of the work was conducted in a facility constructed with support from the NIH, Grant Number C06 RR018823 from the Extramural Research Facilities Program of the National Center for Research Resources.

VI. References

- [1]. Collins KK, Dubin AM, Chiesa NA, Avasarala K, and Van Hare GF, "Cryoablation versus radiofrequency ablation for treatment of pediatric atrioventricular nodal reentrant tachycardia: initial experience with 4-mm cryocatheter," *Heart Rhythm*, vol. 3, no. 5, pp. 564–70, 5, 2006. [PubMed: 16648062]
- [2]. Miyazaki A, Blafox AD, Fairbrother DL, and Saul JP, "Prolongation of the fast pathway effective refractory period during cryoablation in children: a marker of slow pathway modification," *Heart Rhythm*, vol. 2, no. 11, pp. 1179–85, 11, 2005. [PubMed: 16253906]
- [3]. Tuzcu V, "Cryoablation of accessory pathways in children," *Pacing Clin Electrophysiol*, vol. 30, no. 9, pp. 1129–35, 9, 2007. [PubMed: 17725757]
- [4]. Khairy P, Chauvet P, Lehmann J, Lambert J, Macle L, Tanguay JF, Sirois MG, Santoianni D, and Dubuc M, "Lower incidence of thrombus formation with cryoenergy versus radiofrequency catheter ablation," *Circulation*, vol. 107, no. 15, pp. 2045–50, 4 22, 2003. [PubMed: 12668527]
- [5]. Holman WL, Ikeshita M, Ungerleider RM, Smith PK, Ideker RE, and Cox JL, "Cryosurgery for cardiac arrhythmias: acute and chronic effects on coronary arteries," *Am J Cardiol*, vol. 51, no. 1, pp. 149–55, 1 1, 1983. [PubMed: 6849254]
- [6]. Aoyama H, Nakagawa H, Pitha JV, Khammar GS, Chandrasekaran K, Matsudaira K, Yagi T, Yokoyama K, Lazzara R, and Jackman WM, "Comparison of cryothermia and radiofrequency current in safety and efficacy of catheter ablation within the canine coronary sinus close to the left circumflex coronary artery," *J Cardiovasc Electrophysiol*, vol. 16, no. 11, pp. 1218–26, 11, 2005. [PubMed: 16302908]
- [7]. Thomas K, Hans-Peter H, Heike S, Maja K, Jakob S, Anna O, Matthias S, and Thomas P, "Cryoablation at Growing Myocardium: No Evidence of Coronary Artery Obstruction or Intimal Plaque Formation Early and Late after Energy Application," *Pacing and Clinical Electrophysiology*, vol. 32, no. 9, pp. 1197–1202, 2009. [PubMed: 19719499]

- [8]. Lustgarten DL, Keane D, and Ruskin J, "Cryothermal ablation: mechanism of tissue injury and current experience in the treatment of tachyarrhythmias," *Prog Cardiovasc Dis*, vol. 41, no. 6, pp. 481–98, May-Jun, 1999. [PubMed: 10445872]
- [9]. Avari JN, Jay KS, and Rhee EK, "Experience and results during transition from radiofrequency ablation to cryoablation for treatment of pediatric atrioventricular nodal reentrant tachycardia," *Pacing Clin Electrophysiol*, vol. 31, no. 4, pp. 454–60, 4, 2008. [PubMed: 18373764]
- [10]. Chan NY, Mok NS, Lau CL, Lo YK, Choy CC, Lau ST, and Choi YC, "Treatment of atrioventricular nodal re-entrant tachycardia by cryoablation with a 6 mm-tip catheter vs. radiofrequency ablation," *Europace*, vol. 11, no. 8, pp. 1065–70, 8, 2009. [PubMed: 19451097]
- [11]. Gaita F, Montefusco A, Riccardi R, Scaglione M, Grossi S, Caponi D, Caruzzo E, Giustetto C, Bocchiardo M, and Di Donna P, "Acute and long-term outcome of transvenous cryothermal catheter ablation of supraventricular arrhythmias involving the perinodal region," *J Cardiovasc Med*, vol. 7, no. 11, pp. 785–92, 11, 2006.
- [12]. LaPage MJ, Saul JP, and Reed JH, "Long-term outcomes for cryoablation of pediatric patients with atrioventricular nodal reentrant tachycardia," *Am J Cardiol*, vol. 105, no. 8, pp. 1118–21, 4 15, 2010. [PubMed: 20381663]
- [13]. Holman WL, Ikeshita M, Douglas JM Jr., Smith PK, Lofland GK, and Cox JL, "Ventricular cryosurgery: short-term effects on intramural electrophysiology," *Ann Thorac Surg*, vol. 35, no. 4, pp. 386–93, 4, 1983. [PubMed: 6838265]
- [14]. Klein GJ, Harrison L, Ideker RF, Smith WM, Kasell J, Wallace AG, and Gallagher JJ, "Reaction of the myocardium to cryosurgery: electrophysiology and arrhythmogenic potential," *Circulation*, vol. 59, no. 2, pp. 364–72, 2, 1979. [PubMed: 759004]
- [15]. Fedorov VV, Li L, Glukhov A, Shishkina I, Aliev RR, Mikheeva T, Nikolski VP, Rosenshtraukh LV, and Efimov IR, "Hibernator *Citellus undulatus* maintains safe cardiac conduction and is protected against tachyarrhythmias during extreme hypothermia: possible role of Cx43 and Cx45 up-regulation," *Heart Rhythm*, vol. 2, no. 9, pp. 966–75, 9, 2005. [PubMed: 16171752]
- [16]. Smeets JL, Allesie MA, Lammers WJ, Bonke FI, and Hollen J, "The wavelength of the cardiac impulse and reentrant arrhythmias in isolated rabbit atrium. The role of heart rate, autonomic transmitters, temperature, and potassium," *Circ Res*, vol. 58, no. 1, pp. 96–108, 1, 1986. [PubMed: 3943157]
- [17]. Torres JC, and Angelakos ET, "Effect of Hypothermia on Excitation and Propagation in the Isolated Atrium," *Am J Physiol*, vol. 207, pp. 199–202, 7, 1964. [PubMed: 14193590]
- [18]. Leaf DE, Feig JE, Vasquez C, Riva PL, Yu C, Lader JM, Kontogeorgis A, Baron EL, Peters NS, Fisher EA, Gutstein DE, and Morley GE, "Connexin40 imparts conduction heterogeneity to atrial tissue," *Circ Res*, vol. 103, no. 9, pp. 1001–8, 10 24, 2008. [PubMed: 18599871]
- [19]. Steketee J, "Spectral emissivity of skin and pericardium," *Phys Med Biol*, vol. 18, no. 5, pp. 686–94, 9, 1973. [PubMed: 4758213]
- [20]. Pilcher TA, Saul JP, Hlavacek AM, and Haemmerich D, "Contrasting effects of convective flow on catheter ablation lesion size: cryo versus radiofrequency energy," *Pacing Clin Electrophysiol*, vol. 31, no. 3, pp. 300–7, 3, 2008. [PubMed: 18307624]
- [21]. Mistretta CA, Wieben O, Velikina J, Block W, Perry J, Wu Y, and Johnson K, "Highly constrained backprojection for time-resolved MRI," *Magn Reson Med*, vol. 55, no. 1, pp. 30–40, 1, 2006. [PubMed: 16342275]
- [22]. Knisley SB, Justice RK, Kong W, and Johnson PL, "Ratiometry of transmembrane voltage-sensitive fluorescent dye emission in hearts," *Am J Physiol Heart Circ Physiol*, vol. 279, no. 3, pp. H1421–33, 9, 2000. [PubMed: 10993810]
- [23]. Harrison L, Gallagher JJ, Kasell J, Anderson RH, Mikat E, Hackel DB, and Wallace AG, "Cryosurgical ablation of the A-V node-His bundle: a new method for producing A-V block," *Circulation*, vol. 55, no. 3, pp. 463–70, 3, 1977. [PubMed: 837482]
- [24]. Bar-Cohen Y, Cecchin F, Alexander ME, Berul CI, Triedman JK, and Walsh EP, "Cryoablation for accessory pathways located near normal conduction tissues or within the coronary venous system in children and young adults," *Heart Rhythm*, vol. 3, no. 3, pp. 253–8, 3, 2006. [PubMed: 16500293]

- [25]. Gessman LJ, Agarwal JB, Endo T, and Helfant RH, "Localization and mechanism of ventricular tachycardia by ice mapping 1 week after the onset of myocardial infarction in dogs," *Circulation*, vol. 68, no. 3, pp. 657–66, 9, 1983. [PubMed: 6872176]
- [26]. Atienza F, Arenal A, Torrecilla EG, Garcia-Alberola A, Jimenez J, Ortiz M, Puchol A, and Almendral J, "Acute and long-term outcome of transvenous cryoablation of midseptal and parahissian accessory pathways in patients at high risk of atrioventricular block during radiofrequency ablation," *Am J Cardiol*, vol. 93, no. 10, pp. 1302–5, 5 15, 2004. [PubMed: 15135711]
- [27]. Lanzotti ME, De Ponti R, Tritto M, Spadacini G, and Salerno-Uriarte JA, "Successful treatment of anteroseptal accessory pathways by transvenous cryomapping and cryoablation," *Ital Heart J*, vol. 3, no. 2, pp. 128–32, 2, 2002. [PubMed: 11926011]
- [28]. Hunt GB, Chard RB, Johnson DC, and Ross DL, "Comparison of early and late dimensions and arrhythmogenicity of cryolesions in the normothermic canine heart," *J Thorac Cardiovasc Surg*, vol. 97, no. 2, pp. 313–8, 2, 1989. [PubMed: 2915567]
- [29]. Dubuc M, Roy D, Thibault B, Ducharme A, Tardif JC, Villemaire C, Leung TK, and Talajic M, "Transvenous catheter ice mapping and cryoablation of the atrioventricular node in dogs," *Pacing Clin Electrophysiol*, vol. 22, no. 10, pp. 1488–98, 10, 1999. [PubMed: 10588151]
- [30]. Fast VG, Darrow BJ, Saffitz JE, and Kleber AG, "Anisotropic activation spread in heart cell monolayers assessed by high-resolution optical mapping. Role of tissue discontinuities," *Circ Res*, vol. 79, no. 1, pp. 115–27, 7, 1996. [PubMed: 8925559]
- [31]. Wallace AG, and Mignone RJ, "Physiologic evidence concerning the re-entry hypothesis for ectopic beats," *Am Heart J*, vol. 72, no. 1, pp. 60–70, 7, 1966. [PubMed: 4161356]
- [32]. Cavalie A, McDonald TF, Pelzer D, and Trautwein W, "Temperature-induced transitory and steady-state changes in the calcium current of guinea pig ventricular myocytes," *Pflugers Arch*, vol. 405, no. 3, pp. 294–6, 10, 1985. [PubMed: 2415920]
- [33]. Nagatomo T, Fan Z, Ye B, Tonkovich GS, January CT, Kyle JW, and Makielski JC, "Temperature dependence of early and late currents in human cardiac wild-type and long Q-T DeltaKPQ Na⁺ channels," *Am J Physiol*, vol. 275, no. 6 Pt 2, pp. H2016–24, 12, 1998. [PubMed: 9843800]
- [34]. Walsh KB, Begenisich TB, and Kass RS, "Beta-adrenergic modulation of cardiac ion channels. Differential temperature sensitivity of potassium and calcium currents," *J Gen Physiol*, vol. 93, no. 5, pp. 841–54, 5, 1989. [PubMed: 2472462]
- [35]. Bukauskas FF, and Weingart R, "Temperature dependence of gap junction properties in neonatal rat heart cells," *Pflugers Arch*, vol. 423, no. 1-2, pp. 133–9, 4, 1993. [PubMed: 7683787]
- [36]. Shaw RM, and Rudy Y, "Ionic mechanisms of propagation in cardiac tissue. Roles of the sodium and L-type calcium currents during reduced excitability and decreased gap junction coupling," *Circ Res*, vol. 81, no. 5, pp. 727–41, 11, 1997. [PubMed: 9351447]
- [37]. Kuyucak S, and Chung SH, "Temperature dependence of conductivity in electrolyte solutions and ionic channels of biological membranes," *Biophys Chem*, vol. 52, no. 1, pp. 15–24, 9, 1994. [PubMed: 7524714]
- [38]. Einstein A, "On the motion required by the molecular kinetic theory of heat of small particles suspended in a stationary liquid," *Annalen der Physik*, vol. 17, no. 8, pp. 549–560, 1905.

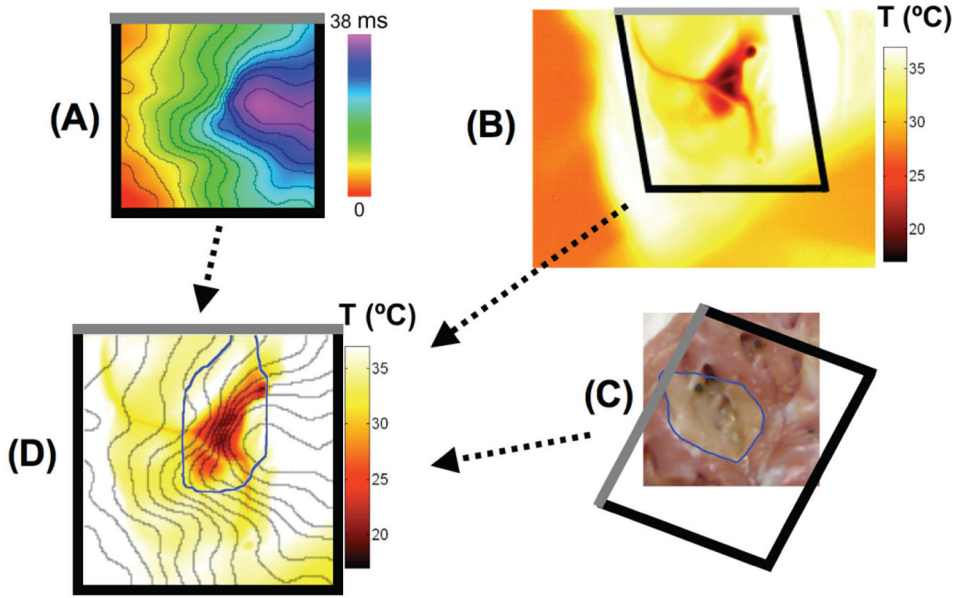


Fig. 1. Registration of three image data sets. (A) Activation map, (B) Epicardial temperature profile after 8 min cryoablation, and (C) Endocardial lesion boundary data are geometrically transformed and registered. Endocardial lesion image is shown flipped horizontally (i.e. as if viewed from the epicardial side) to match the viewing direction of data sets (A) and (B). Original data sets are shown in (A) – (C), with black rectangle (having gray line at top) indicating the region and orientation corresponding between the data sets. (D) Visualization of the registered data sets, where isochrones extracted from (A) are shown at 2.5 ms intervals, endocardial lesion boundary from (C) is shown in blue, and epicardial temperature profile from (B) after 8 min cryoablation is shown as color map. All results are shown from the lesion Endo1.

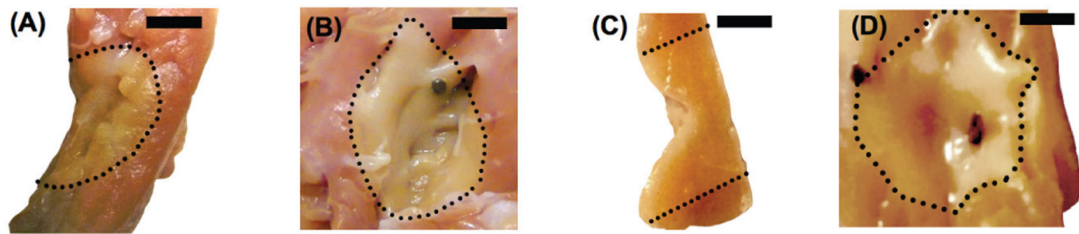


Fig. 2.

Cryo lesion gross pathology. Left ventricular lesion Endo1 (not transmural) in (A) Cross section, and (B) Endocardial view. Right ventricular lesion Endo2 (transmural) in (C) Cross section, and (D) Endocardial view. Protruding fiducials are visible in (B) and (D). Both lesions were created by endocardial cryoablation. Dotted lines mark lesion border. Scale bar indicates 5 mm.

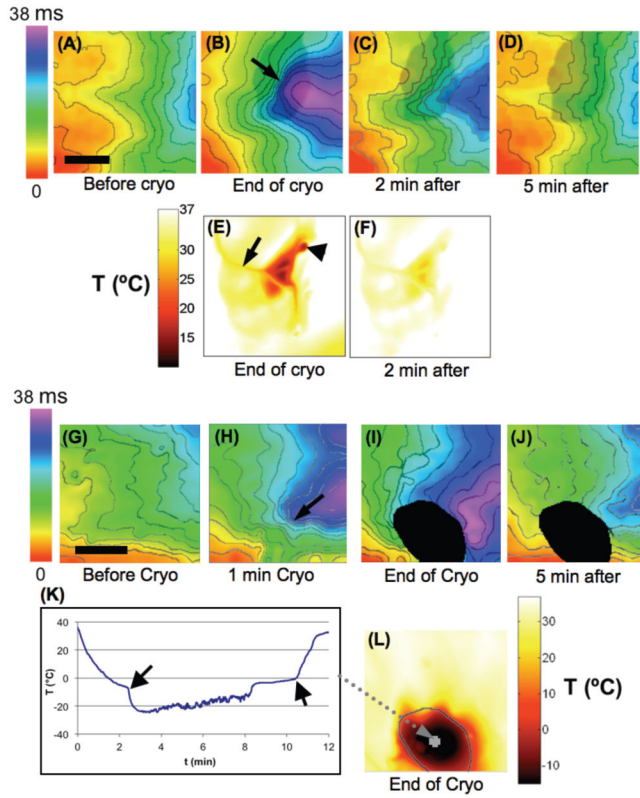


Fig. 3. Conduction changes during non-transmural and transmural cryoablation. Non-transmural lesion (Endo1): Epicardial activation map (A) before, (B) at end of 8 min cryoablation applied endocardially, (C) 2 min after cryo, and (D) 5 min after cryo (see also Suppl. Movie 1). Permanent lesion on the opposite side of the myocardium, i.e. the endocardial side, shown as gray shaded region; isochrones shown at 2.5 ms intervals. Arrow in (B) marks region of conduction block. Epicardial temperature profile is shown (E) at end of 8 min cryoablation, and (F) 2 min after cryo. Coronary vessel (arrow), and fiducial marker (arrowhead) are visible in (E). Tissue was paced from a location at the lower left corner, outside the field of view. Scale bar in (A) indicates 10 mm. Transmural lesion (Endo2): Epicardial activation map (G) before, (H) after 1 min cryoablation applied endocardially (black arrow indicates area of conduction block), (I) at the end of 8 min cryoablation, and (J) 5 min after cryoablation (activation map did not change further after 5 min). (K) Temperature time course in epicardial lesion center (gray marker in (L)), with arrows marking time points of tissue freezing and thawing. (L) Epicardial temperature profile at end of cryoablation (see also Suppl. Movie 2). Permanent lesion (epicardial side) is marked in black in (I) and (J), and by gray outline in (L). Scale bar in (A) indicates 10 mm.

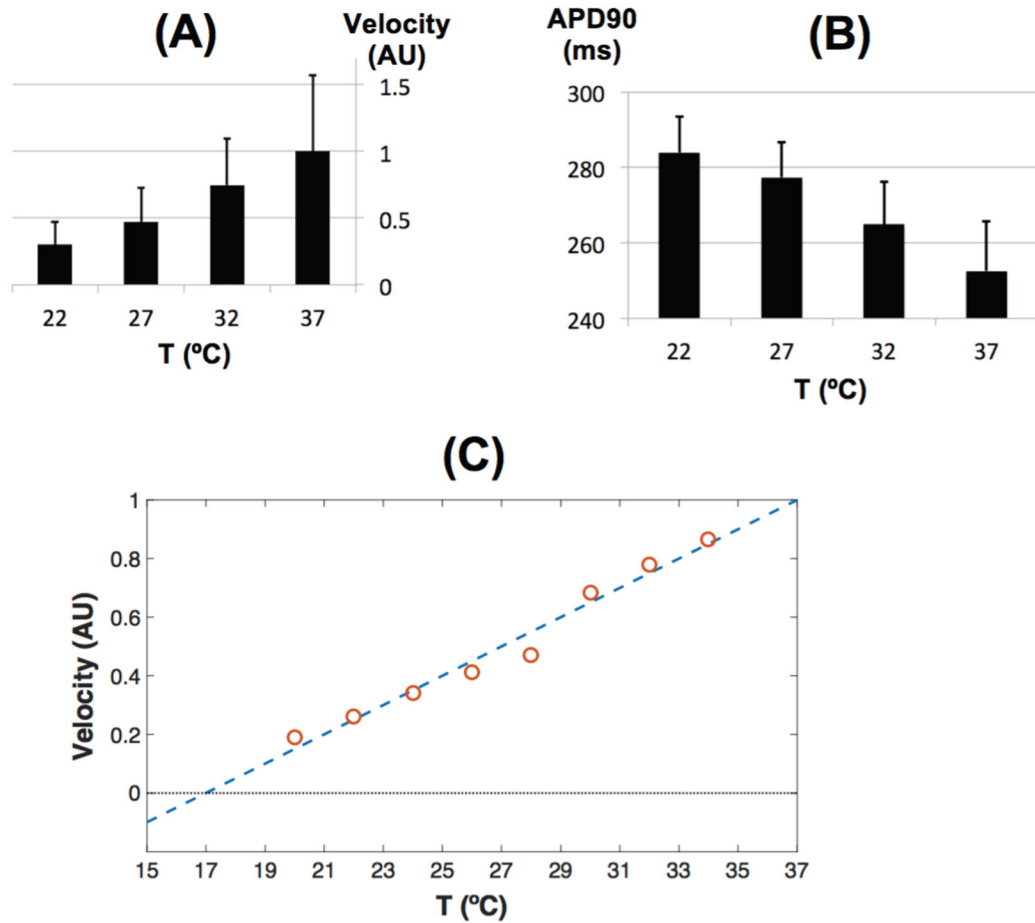


Fig. 4. Temperature dependence of (A) conduction velocity, and of (B) action potential duration (APD90). The temperature coefficient for conduction velocity is $Q_{10}=2.0$. Standard deviation is indicated by bars in (A),(B). (C) Temperature dependence of conduction velocity was used to estimate temperature of conduction block (defined where conduction velocity reaches zero). Blue dashed line indicates linear fit of data (red circles), and intersects with velocity=0 at 17 °C. Based on these data, we estimate transient conduction block to occur at temperatures below 17 °C.

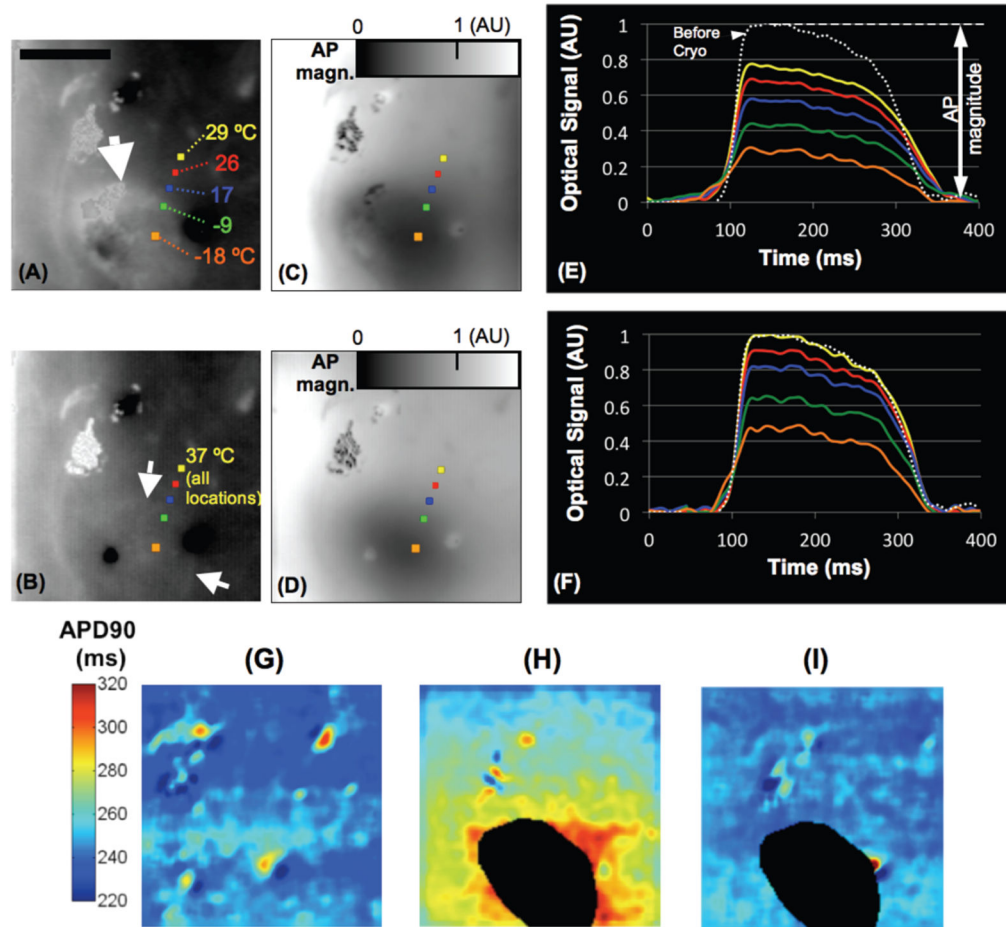


Fig. 5. Temperature dependent changes in action potential morphology. Lesion Endo2: (A) Bright field image, (C) action potential magnitude, and (E) optical signal at indicated locations (corresponding locations indicated by color markers in (A) and (C)). (A), (C) and (E) are shown at the end of the cryoablation. Iceball is visible in (A) and marked by arrow. (B), (D) and (F) show bright field image, action potential magnitude, and optical signal after thawing (5 min after ablation). Permanent lesion is visible in (B) and marked by arrows, coinciding with prior ice ball location in (A). Double arrow in (E) indicates AP magnitude. White dotted curve in (E) and (F) indicates signal before ablation (average signal from all 5 locations). Three fiducial markers are visible in (A) and (B). Before ablation, signals at all locations were equivalent to yellow signal in (F). Scale bar in (A) indicates 10 mm. Action Potential Duration (APD90) map, shown (G) before, (H) at the end of 8 min cryoablation, and (I) 5 min after cryoablation (right). Permanent lesion at epicardial side shown in black in (H) and (I).

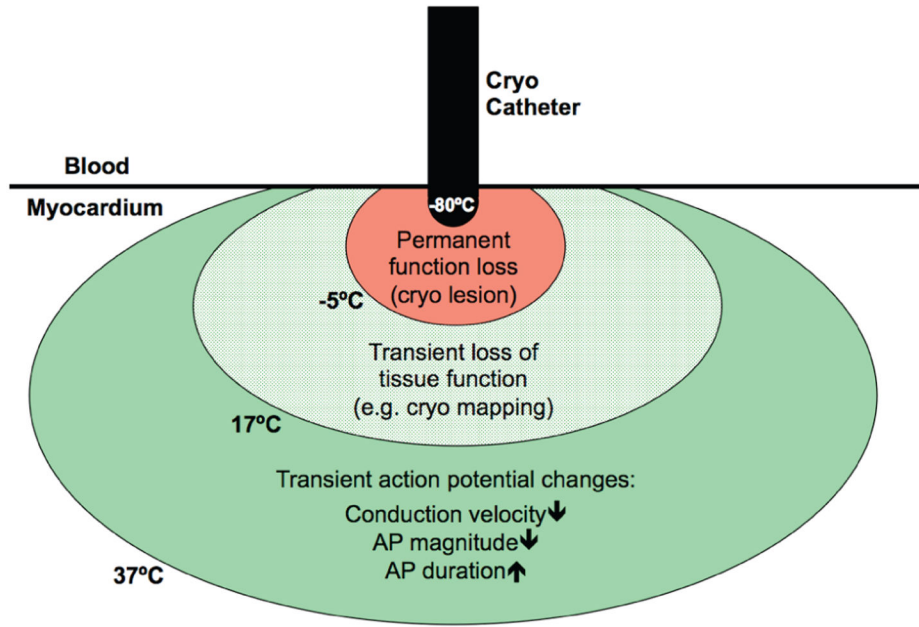


Fig. 6. Tissue effects in proximity of a cryo probe. Three temperature ranges with specific tissue effects have been identified and are simultaneously present. The regions where specific effects occur change dynamically as the cryo probe is cooled down, and heats up again after the end of cryoablation.

TABLE I

Parameter Summary of Cryo Applications

Lesion#	Location	Transmural	Lesion width (mm)	Lesion depth (mm)	Retardation ¹ (ms) [End of cryo]	Retardation ¹ (ms) [After Rewarming]	Lowest Temp ² (°C)	Rewarm time ³ (min)
Epi1	LV	N	18.2	8.9	40	15	<-40	8.6
Epi2	RV	Y	17.4	4.6	15	3	<-40	5.4
Epi3	RV	N	19	4.3	20	5	<-40	5.8
Epi4	RV	Y	13.6	5.9	5	0	<-40	5.5
Endo1	LV	N	15	6.3	25	-1	15	1.4
Endo2	RV	Y	13.6	7.5	21	9	-22	3.4
Endo3	LV	N	13.1	4.8	6	-4	37	NA
Endo4	RV	N	9.6	4.0	25	0	15	2.8

¹ Measured at location of latest activation at end of cryo, as time difference relative to baseline activation time² Infrared camera measurement range limited to temperatures above -40 °C³ Measured from end of cryo application until time when lowest epicardial temperature reached 30 °C